GEOPHYSICAL RESEARCH LETTERS, VOL. 28, NO. 7, PAGES 1179-1182, APRIL 1, 2001

Comparison of measured and modeled stratospheric UV/visible actinic fluxes at large solar zenith angles

Bösch, H.[1], C. Camy-Peyret[2], M. Chipperfield[3], R. Fitzenberger[1], H. Harder[1,4,7], C. Schiller[5], M. Schneider[1,6], T. Trautmann[4,9], and K. Pfeilsticker[1,8]

Abstract. Measured and modeled stratospheric filter sensitivity weighted ultraviolet/visible (UV/vis) actinic fluxes - approximating the NO_2 photolysis rate coefficients (j_{NO_2}) - are compared. The measurements were performed with two calibrated 2π-actinometers assembled on the azimuth angle-controlled LPMA/DOAS (Laboratoire de Physique Moléculaire et Applications / Differential Optical Absorption Spectroscopy) gondola during a series of balloon flights. Since the actinometer's spectral sensitivity curve did not exactly match the actinic spectrum of NO_2 and the skylight's spectrum shape changes with atmospheric height and solar illumination, only proxies (proxy-)j_{NO_2} rather than true j_{NO_2} values were monitored during balloon ascents (0-30 km) for solar zenith angle (SZA) $75^o < SZA < 86^o$, and at balloon float altitude during solar occultation ($86^o < SZA < 95^o$). The measured direct and diffuse total proxy-j_{NO_2} values compare excellently with radiative transfer (RT) modeling. That finding allows us to rule out uncertainties in computing UV/vis actinic fluxes as a significant factor in the still insufficient modeling of stratospheric NO_2 at large SZAs.

1. Introduction

The photolysis of NO_2 (j_{NO_2}) is an important factor controlling the partitioning of stratospheric NO_x (NO, NO_2, and NO_3) through the steady state ratio between NO and NO_2 at daytime. Since j_{NO_2} modulates the daytime stratospheric NO_2 concentration, it indirectly affects the rate of HNO_3 formation via the reaction $NO_2+OH+M \longrightarrow HNO_3+M$, and thus the stratospheric NO_x to NO_y ratio. Recent studies indicate that modeled stratospheric NO_x/NO_y ratios may still fall short even by including the recently updated rate reaction coefficients for the NO_2+OH, and HNO_3+OH reactions in the interpretation of the ER-2 measurements at 20 km for SZAs $< 85^o$[e.g., [e.g., *Brown et al.*, 1999; *Gao et al.*, 1999; *DelNegro et al.*, 1999]. In addition, recent investigations showed that for the Arctic winter inferred stratospheric ozone losses (i.e., at large SZAs) are underestimated by stratospheric CTM's [e.g., *Becker et al.*, 2000]. One possible speculation is based on a consideration whether photochemical models tend to underpredict systematically j-values at large SZAs [Markus Rex, priv. comm., 2000].

In order to further investigate the stratospheric NO_x and NO_y chemistry for large SZAs, we will compare modeled and measured profiles from 8 LPMA/DOAS balloon flights of O_3 measured in the UV, visible, and IR channels, NO (IR), NO_2 (UV, visible, and IR channel), $ClONO_2$ (in the IR) and HNO_3 (in the IR) in future publications. The comparisons show some striking discrepancies between measurements and 3D CTM SLIMCAT modeling [e.g., Chipperfield, 1999] for large SZAs ($\sim 90^o$), which can not be easily reconciled to uncertainties existing in the adopted stratospheric NO_x/NO_y photochemistry.

As a first step for unraveling possible causes, we show here that the measured UV/vis actinic fluxes nicely compare with those adopted in the 3D CTM SLIMCAT photochemical model. Since many more measurements are compared with SLIMCAT simulations - including in part those which claim underpredictions of modeled to measured ozone loss rates for high latitude in winter - it is particularly worthwhile to validate SLIMCAT's RT code for large SZAs. Accordingly, we report on a comparison of stratospheric proxy-j_{NO_2} values measured during two balloon flights with RT calculations using two kinds of models.

2. Methodology

Actinic fluxes were measured during 2 LPMA/DOAS balloon flights from León/Spain (42.6° N, 5.7° W) on Nov. 23, 1996, and Esrange/Sweden (67.9° N, 21.1° E) on Feb. 14, 1997. Both flights were conducted under clear skies, however, with a widely differing ground albedo (A). The two filter actinometers assembled on the azimuth angle-controlled LPMA/DOAS balloon gondola were technically similar to those developed by Junkermann et al. [1989] with improvements as given in Schiller et al. [1994]. The actinometers contain a special 2π viewing inlet device that collects the solar radiation from one hemisphere almost independent of the incident angle. Two actinometers of similar type were mounted in a way that each symmetry axis of the 2π inlet domes pointed to the horizon. One actinometer's symmetry axis (index 'for') was pointing to

[1]Institut für Umweltphysik, University of Heidelberg, Heidelberg, Germany
[2]LPMA, CNRS, Université Pierre et Marie Curie, Paris, France
[3]School of the Environment, University of Leeds, Leeds, UK
[4]Max-Planck-Institut für Chemie, Mainz, Germany
[5]FZ-Jülich, Institut für Stratosphärische Chemie, Jülich, Germany
[6]now with Instituto Nacional de Meteorolgia (INM), Santa Cruz de Tenerife, Spain
[7]now with Meteorology Department, Pennstate University, University Park, USA
[8]also with NOAA, Aeronomy Laboratory, Boulder Co, USA
[9]now with Institut für Meteorologie Universität Leipzig, Leipzig, Germany

Paper number 2000GL012134.
0094-8276/01/2000GL012134$05.00

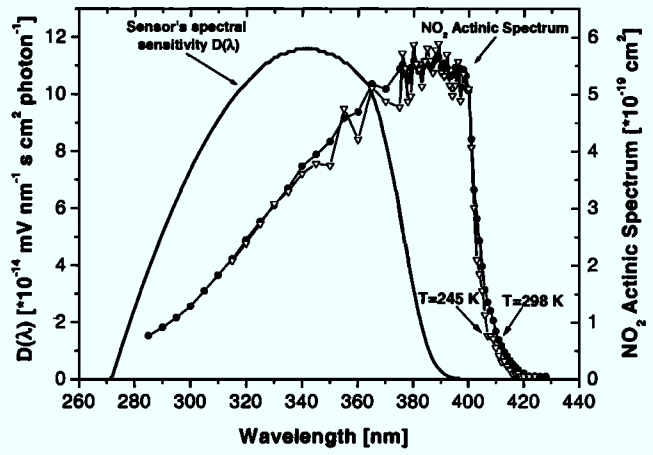

Figure 1. Comparison of the actinic spectrum of NO_2 and the spectral response of the actinometers. For the calculation of the actinic spectrum of NO_2, the quantum yield (Φ) of Roehl et al., [1994] and the NO_2 (σ_{NO_2}) absorption cross section of Davidson et al., [1998] is used. The actinic spectrum of NO_2 is calculated for T = 245 K and 298 K (indicated by open triangles and filled circles, respectively).

the horizon directly into the Sun's azimuthal direction gathering the direct solar radiation (j_{dir}) and the diffuse radiation (j_{diff}) from that part of the hemisphere. The other actinometer (index 'back') was directed to the opposite hemisphere thus only detecting the j_{diff}.

The actinometer's spectral characteristics were fixed to the broad band transmission given by the spectral transmission of Schott UG-11 glasses and the photo tube's spectral sensitivity, that is, from 320 to 400 nm (Figure 1, left y-axis). For a direct comparison with the RT calculations, the absolute spectral sensitivity (units: mV/nm per photons/cm^2/s) of each actinometer was determined in the laboratory with calibrated lamps (1000W, Gigahertz-Optik, type BN-9101-1-PTB) [*Schiller et al.*, 1994]. For calibration, first the relative wavelength dependent spectral sensitivity was measured using a monochromater and a light source. The relative emission spectrum of the system monochromator light source was determined by a calibrated photo diode. In a second step, each actinometer was exposed to the broadband radiation of a calibrated tungsten halogen lamp connected to a processor controlled highly stabilized power supply. The lamps were calibrated by the supplier for several wavelengths traceable to standards of the National Institute for Standards and Technology (NIST) and of the German Physikalisch Technische Bundesanstalt (PTB). The absolute calibration was repeated after each balloon flight in order to correct for possible electronic drifts. The overall accuracy of the actinometer measurements in this wavelength region is about ± 7%.

Since the actinometer's spectral sensitivities do not exactly match the actinic spectrum of NO_2 (Figure 1, right y-axis) , and the skylight spectrum shape changes with height and solar illumination, a fixed actinometer calibration with respect to j_{NO_2} does not exist. However, by knowing the spectrum's shape for each measurement, c.f., from RT modeling, and the sensor's calibration factors as well (see Figure 1 left y-axis), the measured proxy-j_{NO_2} (in units of mV as given in Figure 2) can be directly converted into j_{NO_2} values, 'a posteriori'. Since the purpose of the present study was to test the RT calculations rather than to infer j_{NO_2} values at large SZAs, the spectral sensitivity of each actinometer, rather than the actinic spectrum of NO_2 was used in the RT calculations standing as a surrogate for j_{NO_2} (i.e., the proxy-j_{NO_2}) values.

By knowing the sensor's individually calibrated photoelectrical response (α_{for} and α_{back}, see below), the measured signals S_{for} and S_{back} allow us to infer (proxy-$j_{diff} = \alpha_{back} \times S_{back}$), and proxy-$j_{dir} = \alpha_{for} \times S_{for} - \alpha_{back} \times S_{back}$ assuming that proxy-j_{diff} is the same for both monitored half hemispheres. The above assumption appears to be justified because the diffuse actinic flux in the stratosphere is clearly dominated by the diffuse and almost isotropic back reflection from the Earth's surface (or the cloud cover) and to a lesser extent by the more anisotropic Rayleigh- and Mie scattering of the clear sky atmosphere.

RT model 1 is based on the refined discrete ordinate algorithm (DISORT) [*Kylling and Stamnes*, 1992]. For the low Sun RT calculations, the system of discrete ordinate equations has been modified to incorporate the effect of a spherical shell and refractive atmosphere necessary for the direct beam and primary scattered skylight [*Dahlbeck and Stamnes*, 1991] since atmospheric refraction has shown to be very important for RT modeling for large SZA conditions [*Anderson et al.*, 1986]. The spherical DISORT calculations (16 streams for 196 nm to 505 nm calculated in steps of 1 nm, 70 atmospheric layers of 1 km thickness) were based on the following parameters: the extraterrestrial solar flux from Woods et al. [1996] 196 $nm \leq \lambda \leq$ 410 nm; atmospheric P's and T's, and the O_3 profile were taken from nearby launched ECC sondes, and for z> 30 km data from AFGL for mid-latitudes, and from Anderson et al. [1986] for the subarctic winter; the T-dependent O_3 absorption cross section was taken from Molina and Molina [1986]; the Rayleigh scattering cross section from Nicolet [1984]; the wavelength dependent aerosol extinction β_{aer} profiles from SAGE II measurements (Michael Pitts, priv. comm.) for 15 km<z<30 km; a Henyey-Greenstein phase function and an asymmetry parameter (g) was taken from the MODTRAN optical data base as well as the standard aerosol profiles for $z < 15$ km, but for $z > 30$ km a standard aerosol profiles from Shettle [1989]; for the ground A (not measured directly) the following assumptions were made: for the León flight a mixture of vegetation and pasture with A=0.1, and for the Kiruna flight a snow covered ground providing A=0.7.

The RT model 2 is contained in the SLIMCAT 3D photochemical model. The model calculates the actinic fluxes with a scheme based on Lary and Pyle [1991], which in turn was based on Meier et al. [1982] and Nicolet et al. [1982]. The scheme treats the attenuation of the direct solar beam using full spherical, and refractive geometry for solar zenith angles up to 96°. Enhancement of the solar flux due to multiple scattering is included and is calculated using a plane-parallel atmosphere. In SLIMCAT actinic fluxes are precomputed in a four-dimensional look-up table which has coordinates of pressure altitude, temperature, O_3 column and zenith angles. These tabulated actinic fluxes are interpolated to a particular location in the atmosphere and time. In this study we used local profiles of O_3 and temperature from the appropriate balloon flight up to 30 km and 3D model values for the atmosphere above. The photochemical data used to calculate the j-values were taken from DeMore et al. [1997] and the solar fluxes from WMO [1985]. A fixed 'surface + cloud' A=0.3 was used. In order to account for the larger A of

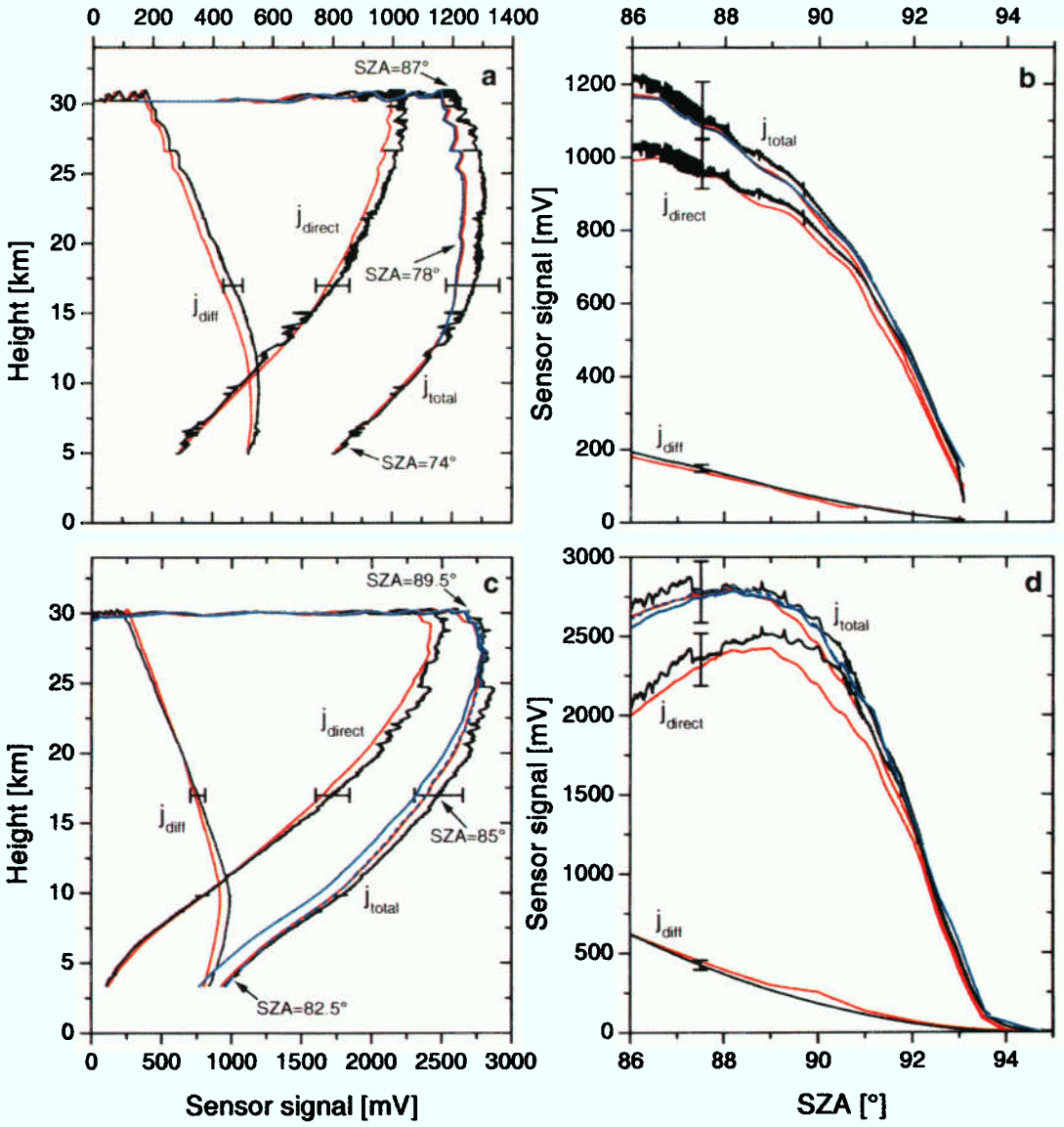

Figure 2. Upper two panels: Comparisons of measured (black lines) and modeled diffuse, direct, and proxy-j_{NO_2} values (DISORT, red lines; LP-RT, blue line for A=0.3), for the León balloon flight on Nov. 23, 1996. Lower two panels: the same but for the Kiruna balloon flight on Feb. 14, 1997 (LP-RT, blue line for A=0.3, and dashed blue line for A=0.7) (left panel balloon ascent, right panel solar for solar occultation). The increase of proxy-j_{NO_2} from SZA=86° to 89° is due to the increase in the balloon flight altitude.

the snow covered ground at Kiruna, a model run with A=0.7 was performed in addition.

3. Results and Discussion

Figure 2 compares the measured and modeled proxy j_{NO_2} values. Though the ground A was different during both flights, it is remarkable that, within the stated experimental errors, the measurements and both RT model calculations agree well for all modes of observation (balloon ascent and solar occultation). This agreement is perhaps less surprising for the DISORT calculations, since more parameters of the individual measurement (e.g., cloud cover, the meteorological parameters and aerosol content) were included than the assumptions (fixed surface and ground A of 0.3 and 0.7, respectively) made in the LP-RT calculations. Obviously, a large ground or tropospheric cloud A significantly increases the calculated stratospheric actinic fluxes at SZA < 90°, as demonstrated here (Figure 2, panel c), or by Madronich et al. [1987]. The upwelling diffuse actinic flux reflected from clouds or the ground adds considerably to the downwelling direct solar actinic flux which usually dominates in the stratosphere (the enhancement being roughly 2×A times the direct solar flux incident on the ground or on the cloud top [*Madronich et al.*, 1997]). Note that the SLIMCAT LP-RT shows better agreement in the range of 5 - 25 km at high latitudes (Figure 2c) when a more realistic of A = 0.7 is assumed. For computational efficiency, a single value is used to set up the photolysis look-up table which, by default, is 0.3. Using a larger A at high latitudes would sightly improve the calculation of proxy-j_{NO_2}.

At large SZA's (>90°), however, a large ground or cloud albedo appears not to be very influential on actinic fluxes in the stratosphere, as the lower parts of the atmosphere and the ground reside in the shadow of

the Earth in this case. Then the stratospheric photolysis is almost completely dominated by the direct solar beam, and the diffuse contribution, primarily due to scattering from the atmosphere (or the ground) below, also becomes low (Figure 2, panels b, and d). Indeed, more detailed computations by Swartz et al. [1999] have shown a 30% increase (at most) of the actinic fluxes at 20 km and a SZA=95° when the ground albedo is increased from 0 to 1. Tropospheric clouds, however, may also have a considerable influence on the actinic fluxes in the stratosphere for large SZA's, just by obscuring the direct solar beam as the Sun sets.

Finally, we note that our measured proxy-j_{NO_2} values can be directly related to j_{NO_2}(within 10%) using the following calibration factors: 7.4×10^{-4}/s/100 mV at SZA=75° for the León flight, and 2.86×10^{-4}/s/100 mV at SZA=83° for the Kiruna flight, respectively. Though the varying importance of Rayleigh scattering and the absorption of ozone may modify somewhat differently the relative contributions of the direct and diffuse actinic fluxes as well as the shape of the spectrum. In practice these calibration factors are accurate to within ± 15% for each of the balloon flights.

4. Summary and Conclusion

Measured and modeled stratospheric proxy-j_{NO_2}(using two independent RT codes) were compared for two completely different geophysical conditions: 1. at mid-latitude and clear sky with low ground albedo, and 2. at high latitudes in winter under clear sky with a snow covered ground providing a large albedo. Overall, the measurements and the RT model calculations agree reasonably and within the stated error bars of the measurements (± 7%,) for all the diffuse, direct, and total proxy-j_{NO_2} values up to SZAs of 94°. So as long as the RT code employs realistic parameters (e.g., albedo (A)), errors of the RT models in calculating stratospheric UV actinic fluxes can be ruled out as considerable source of uncertainty in modeling correctly the stratospheric NO_x and NO_y partitioning, or even the ozone loss rates at very large SZAs.

Acknowledgments.
Support of the project by BMBF (01LO9316/5) and the EU (contracts ENV4-CT-95-0178, and ENV4-CT-97-0524) is gratefully acknowledged. The UK work was supported by the Natural Environment Research Council. We also thank P. Jeseck, T. Hawat, and the team of CNES for the assistance given to perform the balloon flights successfully. Also, we thank A. Kylling and A. Dahlback for fruitful discussions regarding numerical aspects of the pseudo-spherical DISORT. MPC thanks D. Lary for providing his original code. Part of the work was performed while one of the authors (K. Pfeilsticker) held a National Research Council-NOAA Research Associateship.

References

Anderson, G.P., S.A. Clough, F.X. Kneizys, J.H. Chetwynd and E.P. Shettle, AFGL Atmospheric constituent profiles (0-120 km), AFGL-TR-86-0110, AFGL (OPI), Hanscom AFB, MA 01736, 1986.

Becker, G., R. Mueller, D.S. Mc Kenna, M. Rex., K.S. Carlslaw, and H. Oelhaf, Ozone loss rates in the Arctic stratosphere in the winter 19994/95: Model simulations underestimate results of the Match analysis, *J. Geophys,. Res., 105, 15175-15184,* 2000.

Brown, S. S., R. K. Talukdar, and A.R. Ravishankara, Reconsideration of the rate constant for the reaction of hydroxyl radicals with nitric acid, *J. Phys. Chem., 103, 3031 - 3037,* 1999.

Chipperfield, M.P., Multiannual simulations with a 3-D chemical transport model, *J. Geophys. Res.*, 104, 1781-1805, 1999.

Davidson, J.A., C.A.Cantrell, A.H. McDaniel, R.E. Shetter, S. Madronich, and J.G. Calvert, Visible-ultraviolet absorption cross section for NO_2 as a function of temperature, *J. Geophys. Res., 93, 7105-7112,* 1998.

DeMore, W.B., et al., Chemical kinetics and photochemical data for use in stratospheric modeling, *JPL Publ. 97-4,* Jet Propul. Lab., Pasadena, Calif., 1997.

DelNegro, L.A., et al., Comparison of modeled and observed values of NO_2 and j_{NO_2} during the photochemistry of ozone loss in the Arctic region in summer (POLARIS) mission, *J. Geophys. Res., 104, 26,687-26,703,* 1999.

Gao R.S. et al., A comparison of observations and model simulations of NO_x/NO_y in the lower stratosphere, *Geophys. Res. Lett., 26, 1153-1156,* 1999.

Junkermann, W., U. Platt, and A. Volz-Thomas, A photoelectric detector for the measurement of photolysis frequencies of ozone and other atmospheric molecules, *J. Atmos. Chem., 8, 203-227,* 1989.

Kylling, A. and K. Stamnes, Efficient yet accurate solution of the linear transport equation in the presence of internal sources: the exponential-linear approximation, *J. Comp. Phys., 102, 265-276,* 1992.

Lary, D.J., and J.A. Pyle, Diffuse radiation, twilight and photochemistry, *J. Atmos. Chem., 373-392,* 1991.

Madronich, S., Photodissociation in the atmosphere, 1. Actinic flux and the effect of ground reflections and clouds, *J. Geophys. Res., 92, 9740-9752,* 1987.

Meier, R.R., Anderson, D.E. and Nicolet, M., Radiation field in the troposphere and stratosphere from 240 nm - 1000 nm, General Analysis, *Planet. Space Sci., 30, 9, 923-933,* 1982.

Molina, L. T. and M. J. Molina, Absolute absorption cross sections of ozone in the 185 to 350 nm wavelength range, J. *Geophys. Res., 91, 14,501-14,508,* 1986.

Nicolet, M., Meier, R.R., Anderson, D.E., Radiation field in the troposphere and stratosphere from 240 nm - 1000 nm, numerical analysis, *Planet. Space Sci., 30, 9, 935-941,* 1982.

Nicolet, M., On the molecular scattering in the terrestrial atmosphere: An empirical formula for its calculation in the homosphere, *Planet. Space Sci., 32, 1467-1468,* 1984.

Roehl, C.M. J.J. Orlando, G.S. Tyndall, R.E. Shetter, G. J. Vazquez, C.A. Cantrell, and J.G. Calvert, Temperature dependence of the quantum yields for the photolysis of NO_2 near the dissociation limit, *J. Phys. Chem., 98, 7837-7843,* 1994.

Schiller, C., A. Hofzumahaus, M. Müller, E. Klein, E.-P. Röth, and U. Schmidt, Ultraviolet actinic flux in the stratosphere: An overview of balloon-borne measurements during the EASOE, 1991/92, *Geophys. Res. Lett., 21, 1239-1242,* 1994.

Swartz, W. H., S. A. Lloyd, T.L. Kusterer, D.E. Anderson, C.T. McElroy, and C. Midwinter, A sensitivity study of photolysis rate coefficients during POLARIS, *J. Geophys. Res., 26725 - 26735,* 1999.

Shettle, E. P., Models of aerosols, clouds and precipitation for atmospheric propagation studies. Paper presented at Conference on Atmospheric Propagation in the UV, Visible, IR and MM-Region and Related Aspects, NATO Adv. Group for Aerosp. Res. and Dev. Copenhagen, Denmark, 9 - 13 October, 1989.

Woods, T. N. et al., Validation of the UARS solar ultraviolet irradiances: Comparison with the Atlas 1 and 2 measurements, *J. Geophys. Res., 101, 9541-9569,* 1996.

World Meteorological Organization (WMO), *Atmospheric Ozone 1985.* Global Ozone Research and Monitoring Project, Report No. 16, Volume 1, Geneva, Switzerland, 1996.

Bösch et al., Institut für Umweltphysik, Universität Heidelberg, INF 229, D-69120 Heidelberg, Germany (e-mail: hartmut.boesch@iup.uni-heidelberg.de)

(Received July 28, 2000; revised October 13, 2000; accepted January 2, 2001.)